



# Uncertainty assessment of source attribution of PM<sub>2.5</sub> and its water-soluble organic carbon content using different biomass burning tracers in positive matrix factorization analysis – a case study in Beijing, China



Jun Tao <sup>a,b,d,\*</sup>, Leiming Zhang <sup>c</sup>, Renjian Zhang <sup>a,\*</sup>, Yunfei Wu <sup>a</sup>, Zhisheng Zhang <sup>b</sup>, Xiaoling Zhang <sup>e</sup>, Yixi Tang <sup>e</sup>, Junji Cao <sup>d</sup>, Yuanhang Zhang <sup>f</sup>

<sup>a</sup> RCE-TEA, Institute of Atmospheric Physics, Chinese Academy of Sciences, Beijing, China

<sup>b</sup> South China Institute of Environmental Sciences, Ministry of Environmental Protection, Guangzhou, China

<sup>c</sup> Air Quality Research Division, Science Technology Branch, Environment Canada, Toronto, Canada

<sup>d</sup> Key Laboratory of Aerosol Chemistry and Physics, Institute of Earth Environment, Chinese Academy of Sciences, Xi'an, China

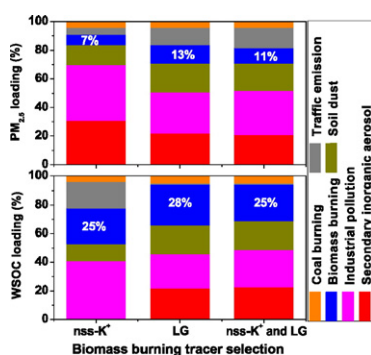
<sup>e</sup> Environmental Meteorology Forecast Center of Beijing-Tianjin-Hebei, Chinese Meteorological Administration, Beijing, China

<sup>f</sup> College of Environmental Sciences and Engineering, Peking University, Beijing, China

## HIGHLIGHTS

- Various biomass burning tracers were compared.
- PM<sub>2.5</sub> source profiles were compared using different biomass burning tracers.
- Uncertainties in source attribution of PM<sub>2.5</sub> and WSOC were quantified.

## GRAPHICAL ABSTRACT



## ARTICLE INFO

### Article history:

Received 15 September 2015

Received in revised form 11 November 2015

Accepted 11 November 2015

Available online 18 November 2015

Editor: D. Barcelo

### Keywords:

Source apportionment  
Biomass burning tracers  
Source profiles

## ABSTRACT

Daily PM<sub>2.5</sub> samples were collected at an urban site in Beijing during four one-month periods in 2009–2010, with each period in a different season. Samples were subject to chemical analysis for various chemical components including major water-soluble ions, organic carbon (OC) and water-soluble organic carbon (WSOC), element carbon (EC), trace elements, anhydrosugar levoglucosan (LG), and mannosan (MN). Three sets of source profiles of PM<sub>2.5</sub> were first identified through positive matrix factorization (PMF) analysis using single or combined biomass tracers – non-sea salt potassium (nss-K<sup>+</sup>), LG, and a combination of nss-K<sup>+</sup> and LG. The six major source factors of PM<sub>2.5</sub> included secondary inorganic aerosol, industrial pollution, soil dust, biomass burning, traffic emission, and coal burning, which were estimated to contribute 31 ± 37%, 39 ± 28%, 14 ± 14%, 7 ± 7%, 5 ± 6%, and 4 ± 8%, respectively, to PM<sub>2.5</sub> mass if using the nss-K<sup>+</sup> source profiles, 22 ± 19%, 29 ± 17%, 20 ± 20%, 13 ± 13%, 12 ± 10%, and 4 ± 6%, respectively, if using the LG source profiles, and 21 ± 17%, 31 ± 18%, 19 ± 19%, 11 ± 12%, 14 ± 11%, and 4 ± 6%, respectively, if using the combined nss-K<sup>+</sup> and LG source profiles. The uncertainties in the estimation of biomass burning contributions to WSOC due to the different choices of biomass

\* Corresponding authors at: No. 7, West Street, Yuancun, Guangzhou, China.  
E-mail addresses: [taojun@scies.org](mailto:taojun@scies.org) (J. Tao), [zrj@mail.iap.ac.cn](mailto:zrj@mail.iap.ac.cn) (R. Zhang).

burning tracers were around 3% annually and up to 24% seasonally in terms of absolute percentage contributions, or on a factor of 1.7 annually and up to a factor of 3.3 seasonally in terms of the actual concentrations. The uncertainty from the major source (e.g. industrial pollution) was on a factor of 1.9 annually and up to a factor of 2.5 seasonally in the estimated WSOC concentrations.

© 2015 Elsevier B.V. All rights reserved.

## 1. Introduction

Fine particulate matter with an aerodynamic diameter of less than  $2.5\ \mu\text{m}$  ( $\text{PM}_{2.5}$ ) affects human and ecosystem health and also plays an important role in weather modification and climate change (Ali-Mohamed, 1991; Ali-Mohamed and Ali, 2001; Bell et al., 2007).  $\text{PM}_{2.5}$  is a complex mixture of chemical compounds mainly composing sulfate, nitrate, ammonium, OC, EC, soil dust and water (Seinfeld et al., 2004; Chan and Yao, 2008; Fang and Liu, 2010; Johansen and Hoffmann, 2004; Kumar et al., 2010; Wang et al., 2002; Zhang et al., 2011a). Water-soluble chemical components, including water-soluble inorganic ions and water-soluble organic matter, play more important roles than insoluble ones on aerosols light scattering and their ability of serving as cloud condensation nuclei (Decesari et al., 2003; Du et al., 2014b; Hecobian et al., 2010; Jung et al., 2011; Zhang et al., 2011b).

Dominant water-soluble inorganic ions (sulfate, nitrate, and ammonium) are mainly secondary aerosols forming from their respective gaseous precursors. However, water-soluble organic matter or water-soluble organic carbon (WSOC) can originate from both primary emissions and secondary organic aerosol (SOA) formations, the latter are through the oxidation processes involving volatile organic compounds (VOCs) (Kalberer et al., 2000; Pathak et al., 2011). Biomass burning rather than fossil fuel combustion was considered to be the major primary source for WSOC (Sullivan et al., 2006; Timonen et al., 2010; Wonaschütz et al., 2011; Gordon et al., 2014; Peltier et al., 2007). Thus, WSOC can be a marker for SOA in the absence of biomass burning (Docherty et al., 2008).

LG is a unique organic tracer for biomass burning because the combustion of other fuels seldom produce LG. The disadvantage of using LG as a tracer is its degradation during transportation process which may affect source apportionment results (Fraser and Lakshmanan, 2000; Popovicheva et al., 2014). The inorganic tracer  $\text{K}^+$  has also been used extensively to identify biomass burning (Gieré et al., 2006). Although  $\text{K}^+$  is not an ideal tracer due to its other sources (e.g., soil dust, sea

salt, and coal combustion) (Cheng et al., 2000; Duvall et al., 2008; Ninomiya et al., 2004), it does not degrade during transportation. Moreover, seasonal dependent biomass burning types and their respective emission factors for LG and  $\text{K}^+$  further add difficulties to quantitatively assessing biomass burning contributions to  $\text{PM}_{2.5}$  and WSOC. For example, wheat and rape straws are burned in spring, rice and corn straws in autumn and woods in winter (Cheng et al., 2013; Tao et al., 2013, 2014; Wang et al., 2007; Zhang et al., 2015). Therefore, choice of biomass burning tracers could lead to some uncertainties when estimating the contribution of biomass burning to  $\text{PM}_{2.5}$  and WSOC.

A previous study using LG as a tracer of biomass burning suggested that biomass burning accounted for 40% of WSOC in Beijing (Du et al., 2014a). However, the uncertainties in source attribution analysis by different biomass burning tracers are unknown. To assess the sources especially biomass burning contributing to  $\text{PM}_{2.5}$  and WSOC in Beijing, a comprehensive data set acquired in 2009–2010 is analyzed in the present study making use of previously generated  $\text{PM}_{2.5}$  source profiles for this city. The study aims to accomplish the following goals: (1) to systematically characterize WSOC levels on seasonal and annual basis; (2) to identify the biomass burning profiles based on chemical components in  $\text{PM}_{2.5}$  using various biomass burning tracers; and (3) to quantify the contributions of biomass burning to  $\text{PM}_{2.5}$ , WSOC and potential uncertainties in the PMF results due to choices of different biomass burning tracers. Biomass burning tracers  $\text{nss-K}^+$ , LG, and a combination of  $\text{nss-K}^+$  and LG are applied separately to PMF analysis to quantify the uncertainties in source attribution analysis.

## 2. Methodology

### 2.1. Site description

$\text{PM}_{2.5}$  samples were collected at the Peking University (PKU) ( $39.99^\circ\text{N}$ ,  $116.30^\circ\text{E}$ ) located in the urban area of Beijing (Fig. 1). Instruments

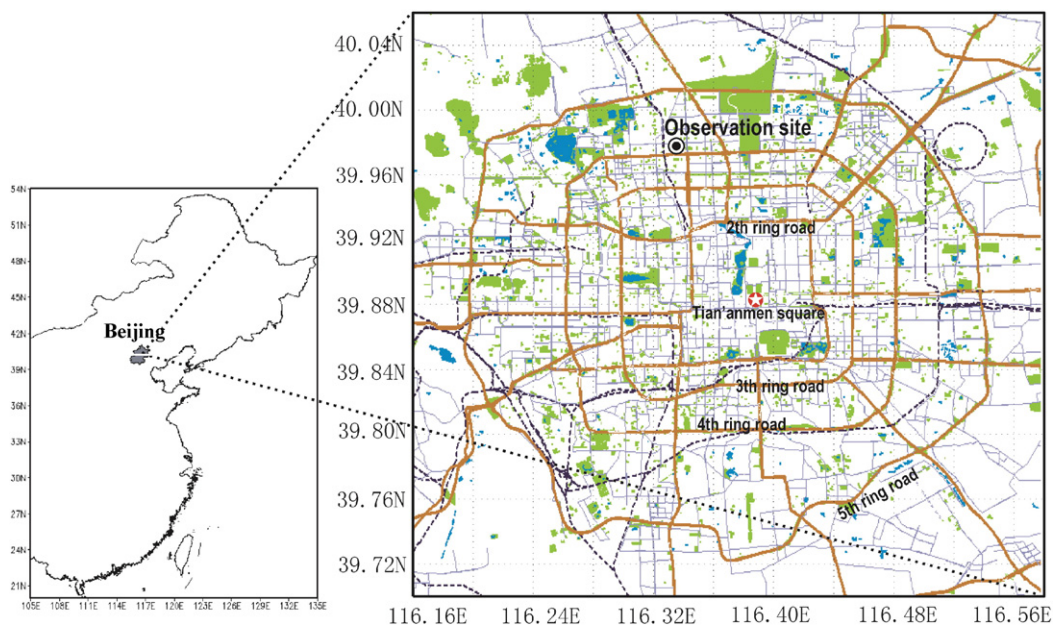


Fig. 1. The sampling location ( $40^{\circ}02'\text{N}$ ,  $116^{\circ}24'\text{E}$ ) in Beijing.

used in this study were installed on the roof (26 m above ground) of an office building of the PKU. This site is located within the educational, commercial, and residential districts, and no main pollution sources exist nearby. Thus, the observations could represent typical pollution conditions in an urban environment of Beijing (Zhang et al., 2013).

## 2.2. Sampling

PM<sub>2.5</sub> samples were collected using two low-flow air samplers (from OMNI™, BGI, USA). Prior to the start of the sampling campaign, the flow rate of PM<sub>2.5</sub> samplers was calibrated. Samples were collected at a flow rate of 5 L min<sup>-1</sup> on two types of filters: 47 mm quartz fiber filter (Whatman QM-A) and 47 mm Teflon filter (Whatman PTFE). Quartz filters were pre-baked at 800 °C for 3 h prior to sampling. Collected filters were stored in a freezer at -18 °C before chemical analysis to minimize evaporation of volatile components.

A total of 119 PM<sub>2.5</sub> samples and 8 blank samples were collected in 2009–2010 during the following periods: 1–30 April 2009 (representative of spring), 1–31 July 2009 (summer), 1–31 October 2009 (autumn)

and 1–31 January 2010 (winter). Collection duration of each sample was 24 h, starting at 10:00 local time each day and ending at 10:00 the following day. Field blanks were collected with each sampler during every seasonal campaign, which were then analyzed together with the samples.

## 2.3. Gravimetric weighing

Teflon filters were measured gravimetrically for particle mass concentrations using a Sartorius MC5 electronic microbalance with a sensitivity of ±1 µg (Sartorius, Göttingen, Germany) after 24 h equilibration at 23 ± 1 °C with relative humidity at 40 ± 5%. Each filter was weighed at least three times both before and after sampling. Differences among replicate weights were mostly less than 20 µg for each sample. Net mass was obtained by subtracting pre-weight from post-weight. The limit of detection (LOD) of microbalance was 1 µg. The LOD of PM<sub>2.5</sub> mass concentration was around 0.14 µg m<sup>-3</sup>. The net mass of samples ranged from 282 to 2554 µg. Thus, the uncertainty of PM<sub>2.5</sub> mass concentration ranged from 2% to 7%.

**Table 1**  
Annual and seasonal statistics of PM<sub>2.5</sub> and its chemical components, gaseous pollutants and meteorological variables in Beijing.

	Annual (n = 119)	Spring (n = 29)	Summer (n = 29)	Autumn (n = 31)	Winter (n = 30)
PM <sub>2.5</sub> (µg m <sup>-3</sup> )	135 ± 63	126 ± 59	138 ± 48	135 ± 55	139 ± 86
OC (µgC m <sup>-3</sup> )	16.9 ± 10.0	13.7 ± 4.4	11.1 ± 1.8	17.8 ± 5.6	24.9 ± 15.6
EC (µgC m <sup>-3</sup> )	5.0 ± 4.4	2.8 ± 1.1	4.2 ± 1.2	5.3 ± 2.8	7.5 ± 7.4
WSOC (µgC m <sup>-3</sup> )	6.4 ± 3.6	6.7 ± 1.8	3.2 ± 1.1	7.7 ± 5.0	7.7 ± 3.6
Na <sup>+</sup> (µg m <sup>-3</sup> )	0.5 ± 0.6	0.3 ± 0.2	0.2 ± 0.1	0.3 ± 0.2	1.1 ± 0.8
NH <sub>4</sub> <sup>+</sup> (µg m <sup>-3</sup> )	6.9 ± 7.1	7.7 ± 8.2	10.9 ± 6.9	4.7 ± 5.8	4.5 ± 5.7
K <sup>+</sup> (µg m <sup>-3</sup> )	0.9 ± 0.8	1.1 ± 0.7	0.6 ± 0.5	1.1 ± 0.9	0.8 ± 0.8
nss-K <sup>+</sup> (µg m <sup>-3</sup> )	0.9 ± 0.7	1.0 ± 0.7	0.6 ± 0.5	1.1 ± 0.9	0.8 ± 0.8
Mg <sup>2+</sup> (µg m <sup>-3</sup> )	0.2 ± 0.1	0.2 ± 0.2	0.1 ± 0.0	0.2 ± 0.1	0.2 ± 0.1
Ca <sup>2+</sup> (µg m <sup>-3</sup> )	1.6 ± 1.5	2.7 ± 2.2	0.7 ± 0.4	1.7 ± 1.0	1.5 ± 0.9
Cl <sup>-</sup> (µg m <sup>-3</sup> )	1.4 ± 2.2	0.7 ± 0.8	0.3 ± 0.6	1.1 ± 1.0	3.5 ± 3.3
NO <sub>3</sub> <sup>-</sup> (µg m <sup>-3</sup> )	11.3 ± 10.8	15.9 ± 13.7	11.5 ± 8.2	10.7 ± 11.0	7.3 ± 8.1
SO <sub>4</sub> <sup>2-</sup> (µg m <sup>-3</sup> )	13.5 ± 12.4	15.1 ± 11.5	23.2 ± 14.7	7.9 ± 7.4	8.5 ± 8.6
LG (ng m <sup>-3</sup> )	203 ± 229	74 ± 44	28 ± 17	385 ± 213	311 ± 262
MN (ng m <sup>-3</sup> )	20 ± 24	7 ± 5	5 ± 3	23 ± 13	43 ± 34
Al (ng m <sup>-3</sup> )	1823 ± 1493	2465 ± 1733	691 ± 427	2009 ± 1412	2106 ± 1454
Fe (ng m <sup>-3</sup> )	1696 ± 1080	1933 ± 1175	945 ± 715	2052 ± 1038	1826 ± 1018
Na (ng m <sup>-3</sup> )	766 ± 602	636 ± 266	334 ± 123	630 ± 292	1451 ± 772
Mg (ng m <sup>-3</sup> )	718 ± 554	937 ± 637	273 ± 178	867 ± 574	784 ± 461
K (ng m <sup>-3</sup> )	1608 ± 914	1841 ± 872	1045 ± 697	1959 ± 983	1566 ± 833
Ca (ng m <sup>-3</sup> )	2387 ± 2023	3380 ± 2641	904 ± 645	2960 ± 1929	2269 ± 1455
Sr (ng m <sup>-3</sup> )	16 ± 12	18 ± 13	6 ± 3	16 ± 10	24 ± 13
Ba (ng m <sup>-3</sup> )	34 ± 22	41 ± 25	15 ± 07	39 ± 19	39 ± 23
Ti (ng m <sup>-3</sup> )	130 ± 97	162 ± 107	53 ± 33	152 ± 97	151 ± 95
Mn (ng m <sup>-3</sup> )	78 ± 37	78 ± 33	42 ± 17	92 ± 34	101 ± 33
Ni (ng m <sup>-3</sup> )	4 ± 2	4 ± 3	2 ± 1	4 ± 2	6 ± 3
Cu (ng m <sup>-3</sup> )	34 ± 23	36 ± 26	33 ± 22	33 ± 20	33 ± 26
Zn (ng m <sup>-3</sup> )	270 ± 164	279 ± 177	265 ± 123	310 ± 160	223 ± 186
Mo (ng m <sup>-3</sup> )	1 ± 1	1 ± 1	1 ± 0	1 ± 1	2 ± 1
Cd (ng m <sup>-3</sup> )	3 ± 2	3 ± 3	3 ± 3	3 ± 2	2 ± 3
Sn (ng m <sup>-3</sup> )	9 ± 7	10 ± 7	9 ± 6	10 ± 6	9 ± 8
Sb (ng m <sup>-3</sup> )	10 ± 7	9 ± 6	8 ± 5	10 ± 6	11 ± 10
Tl (ng m <sup>-3</sup> )	2 ± 2	2 ± 1	2 ± 1	2 ± 1	3 ± 2
Pb (ng m <sup>-3</sup> )	143 ± 99	137 ± 91	121 ± 75	147 ± 99	168 ± 123
V (ng m <sup>-3</sup> )	4 ± 3	5 ± 2	2 ± 1	5 ± 3	5 ± 3
Cr (ng m <sup>-3</sup> )	11 ± 9	9 ± 5	8 ± 4	17 ± 13	10 ± 10
As (ng m <sup>-3</sup> )	11 ± 14	12 ± 13	19 ± 22	8 ± 6	8 ± 6
Se (ng m <sup>-3</sup> )	3 ± 2	4 ± 3	4 ± 2	3 ± 2	3 ± 2
Zr (ng m <sup>-3</sup> )	6 ± 4	7 ± 5	2 ± 1	6 ± 4	8 ± 5
Ge (ng m <sup>-3</sup> )	1 ± 2	1 ± 0	1 ± 0	1 ± 0	4 ± 3
Rb (ng m <sup>-3</sup> )	9 ± 5	10 ± 5	6 ± 4	11 ± 6	9 ± 4
Cs (ng m <sup>-3</sup> )	1 ± 1	1 ± 1	1 ± 1	1 ± 1	1 ± 1
Ga (ng m <sup>-3</sup> )	5 ± 5	4 ± 2	2 ± 1	4 ± 2	10 ± 7
SO <sub>2</sub> (µg m <sup>-3</sup> )	33 ± 44	21 ± 13	10 ± 8	15 ± 7	88 ± 60
O <sub>3</sub> (µg m <sup>-3</sup> )	41 ± 33	65 ± 16	75 ± 27	18 ± 9	17 ± 14
NO <sub>2</sub> (µg m <sup>-3</sup> )	54 ± 28	49 ± 18	40 ± 10	67 ± 26	64 ± 45
SR (MJ m <sup>-2</sup> )	14 ± 6	19 ± 6	17 ± 5	12 ± 4	8 ± 3
RH (%)	50 ± 16	43 ± 16	68 ± 9	49 ± 16	42 ± 15

## 2.4. Chemical analysis

Water-soluble organic carbon (WSOC) was analyzed by a Sievers 900 TOC analyzer (GE Analytical, U.S.A.). Anhydrosugar LG and MN were measured by a Dionex ICS-3000 system. Water-soluble ions including  $F^-$ ,  $Cl^-$ ,  $NO_3^-$ ,  $SO_4^{2-}$ ,  $Na^+$ ,  $NH_4^+$ ,  $K^+$ ,  $Mg^{2+}$  and  $Ca^{2+}$  were analyzed by a Dionex model ICS-90 (for anions) and ICS-1500 (for cations) ion chromatograph. OC and EC were analyzed by a DRI model 2001 carbon analyzer (Atmoslytic, Inc., Calabasas, CA, USA). Trace elements were analyzed by an inductively coupled plasma-mass spectrometry (ICP-MS). A detailed description of the analytical method can be found in Tao et al. (2013) and Zhang et al. (2013).

## 2.5. Data analysis methods

Source apportionment analysis was conducted using positive matrix factorization (PMF) Model Version 5.0 of U.S. Environmental Protection Agency (EPA) (Norris et al., 2014). To reduce uncertainties of PMF results, chemical components with annual average concentrations below method detection limits (MDLs) were removed. Thirty-nine chemical components were used for the PMF model, including WSOC, water-insoluble organic carbon (WIOC), EC, LG,  $Na^+$ ,  $NH_4^+$ ,  $K^+$ ,  $Mg^{2+}$ ,  $Ca^{2+}$ ,  $Cl^-$ ,  $NO_3^-$ ,  $SO_4^{2-}$ , Al, Fe, Sr, Ba, Ti, Mn, Co, Ni, Cu, Zn, Mo, Cd, Sn, Sb, Tl, Pb, V, Cr, As, Se, Zr, Ge, Rb, Cs, Ga, La, Ce and Nd (Table 1).  $K^+$  concentrations presented here were corrected by a sea salt indicator ( $Mg^{2+}$ ), i.e.,  $nss-K^+ = K^+ - 0.159 Mg^{2+}$  (Cheng et al., 2000). Method detection limits (MDL) were within the range of 0.01 to 0.04  $\mu g m^{-3}$  for cations, 0.03 to 0.07  $\mu g m^{-3}$  for anions, 0.02  $\mu g m^{-3}$  for OC and EC; 0.06  $\mu g m^{-3}$  for WSOC; 0.1 to 1.0  $ng m^{-3}$  for elements, and 0.57  $ng m^{-3}$  for sugars. The uncertainties should be less than 5% for ions and sugars, 10% for OC, EC and WSOC, and 10–15% for elements. Here, WIOC concentrations equaled to OC minus WSOC and the uncertainties of WIOC were estimated by the uncertainties of OC and WSOC.

To determine the appropriate number of source factors, a reasonable practice is to test different numbers of identifiable sources commonly used and to consider the major potential sources documented by the previous study (Zhang et al., 2013). According to the results of PMF, the correlation between simulated and measured Cr and As were poor ( $R^2 < 0.4$ ,  $R^2 > 0.6$  for other chemical species). Thus, we removed the two elements in PMF model. Finally, six main source factors were identified, including secondary inorganic aerosol, industrial pollution, soil dust, biomass burning, traffic emission, and coal burning based on the similar database with Zhang et al. (2013). Then, PMF was run several

times with different  $F_{peak}$  values to determine the range within which the objective function Q values remain relatively constant. In the six-factor model, a value of  $F_{peak} = -0.1$  provided the most physically reasonable source profiles.

## 2.6. Meteorological parameters and routine air pollutants

Meteorological parameters, including relative humidity (RH) and solar radiation (SR) were collected from Beijing meteorology stations (39°48'N, 116°28'E). Trace gases including sulfur dioxide ( $SO_2$ ) and nitrogen dioxide ( $NO_2$ ) and  $PM_{10}$  (aerosol particles with an aerodynamic diameter of less than 10  $\mu m$ ) were collected at the Wanliu national environmental monitoring site, which is located 2.0 km southwest of the PKU site. Ozone ( $O_3$ ) was collected at the Baolian Sports Park site (Zhao et al., 2009), which is located 6.0 km southwest of the PKU site. The two sites are located between the third and the fourth Ring Road in the western urban area of Beijing.

## 3. Results and discussion

### 3.1. Characteristics of WSOC in $PM_{2.5}$

The annual average  $PM_{2.5}$ , OC, EC, and WSOC were  $135 \pm 63 \mu g m^{-3}$ ,  $16.9 \pm 10.0 \mu g C m^{-3}$ ,  $5.0 \pm 4.4 \mu g C m^{-3}$ , and  $6.4 \pm 3.6 \mu g C m^{-3}$ , respectively (Table 1). OC and EC accounted for  $13.2 \pm 4.7\%$  and  $3.5 \pm 1.4\%$  (expressed as  $\mu g C \mu g^{-1}$ ), respectively, of  $PM_{2.5}$  mass. WSOC accounted for  $38.7 \pm 13.1\%$  of OC and  $5.1 \pm 2.3\%$  of  $PM_{2.5}$  ( $\mu g C \mu g^{-1}$ ). The annual value of WSOC was comparable to that ( $7.2 \pm 5.5 \mu g C m^{-3}$ ) based on thirteen months measurement in 2010–2011 in Beijing (Du et al., 2014a). However, the value was evidently higher than that ( $2.0 \mu g C m^{-3}$ ) measured in Guangzhou (Huang et al., 2012).

The seasonal patterns of WSOC were similar to those of OC (Table 1), with the highest seasonal average concentration in winter ( $7.7 \pm 3.6 \mu g C m^{-3}$ ) and autumn ( $7.7 \pm 5.0 \mu g C m^{-3}$ ), relatively high concentration in spring ( $6.7 \pm 1.8 \mu g C m^{-3}$ ), and the lowest in summer ( $3.2 \pm 1.1 \mu g C m^{-3}$ ). Seasonal averages WSOC in winter, autumn and spring were all more than doubled that in summer. The seasonal average WSOC concentrations in this study were lower than those measured in 2010–2011 in Beijing, Shanghai and Indo-Gangetic Plain of India (Du et al., 2014a; Pathak et al., 2011; Ram and Sarin, 2011) and were higher than those measured in Guangzhou, Seoul of Korea (Park et al., 2012), European cities (e.g. Amsterdam, Barcelona and Ghent) (Viana et al., 2007) and American cities (e.g. North Birmingham, Centreville

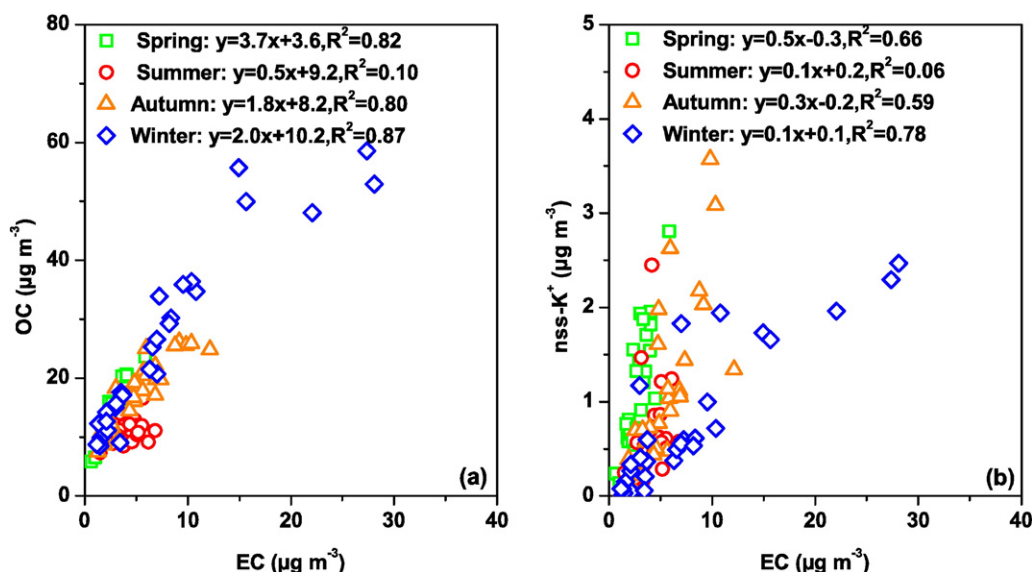


Fig. 2. Scatter plots of OC versus EC (a) and  $nss-K^+$  versus EC (b).

and Pensacola) (Ding et al., 2008) in the same seasons. WSOC concentrations in Beijing were on the high-end levels in the world.

Seasonal averages WSOC in  $PM_{2.5}$  in spring ( $6.0 \pm 2.4\%$ ,  $\mu\text{gC } \mu\text{g}^{-1}$ ), autumn ( $5.9 \pm 1.5\%$ ,  $\mu\text{gC } \mu\text{g}^{-1}$ ) and winter ( $5.7 \pm 2.3\%$ ,  $\mu\text{gC } \mu\text{g}^{-1}$ ) were also more than doubled that in summer ( $2.6 \pm 1.0\%$ ,  $\mu\text{gC } \mu\text{g}^{-1}$ ), similar to what was found in seasonal WSOC concentrations. Small differences in the seasonal patterns of WSOC and WSOC/ $PM_{2.5}$  ratio should be caused by seasonal variations of WSOC sources strength as further discussed in Section 3.4.

### 3.2. Identification of biomass burning using various tracers

Levoglucosan (LG) concentrations in autumn ( $385 \pm 213 \text{ ng m}^{-3}$ ) and winter ( $311 \pm 262 \text{ ng m}^{-3}$ ) were 4 to 14 times higher than those in spring ( $74 \pm 44 \text{ ng m}^{-3}$ ) and summer ( $28 \pm 17 \text{ ng m}^{-3}$ ). Seasonal variations in  $nss\text{-K}^+$  concentrations were less than a factor of 2.0 with the highest concentration in spring ( $1.0 \pm 0.7 \mu\text{g m}^{-3}$ ) and autumn ( $1.1 \pm 0.9 \mu\text{g m}^{-3}$ ), relatively high concentration in winter ( $0.8 \pm 0.8 \mu\text{g m}^{-3}$ ), and the lowest concentration in summer ( $0.6 \pm 0.5 \mu\text{g m}^{-3}$ ). Thus, both LG and  $nss\text{-K}^+$  tracers confirmed the biomass

burning sources of carbonaceous aerosols in autumn and winter. However, these two tracers do not agree with each other in spring, which could be a result of significant losses in LG and/or additional sources of  $nss\text{-K}^+$ .

Besides LG and  $nss\text{-K}^+$ , other tracers used in literature include OC/EC and  $nss\text{-K}^+/\text{EC}$  ratios, which vary substantially from different sources. For example, OC/EC ratio has been identified for coal combustion (0.3–7.6), vehicle emission (0.7–2.4), and biomass burning (4.1–14.5) (Watson et al., 2001), and  $nss\text{-K}^+/\text{EC}$  ratio has been identified for biomass burning (0.2 to 0.5) and fossil fuel combustion (0.03–0.09) (Andreae, 1983; Popovicheva et al., 2014). These tracers are compared below using data collected in this study. Seasonal average OC/EC ratios were 3.7, 0.5, 1.8 and 2.0 and  $nss\text{-K}^+/\text{EC}$  ratios were 0.5, 0.1, 0.3 and 0.1 in spring, summer, autumn and winter, respectively (see regression equations in Fig. 2). The highest ratios for both OC/EC and  $nss\text{-K}^+/\text{EC}$  in spring suggested biomass burning to be an important source of carbonaceous aerosols. The much lower LG concentrations in spring than in autumn and winter suggested substantial loss of LG in spring, knowing that biomass burning emissions are high in spring. The low LG in summer may due to a combination of LG loss and low emission rates in

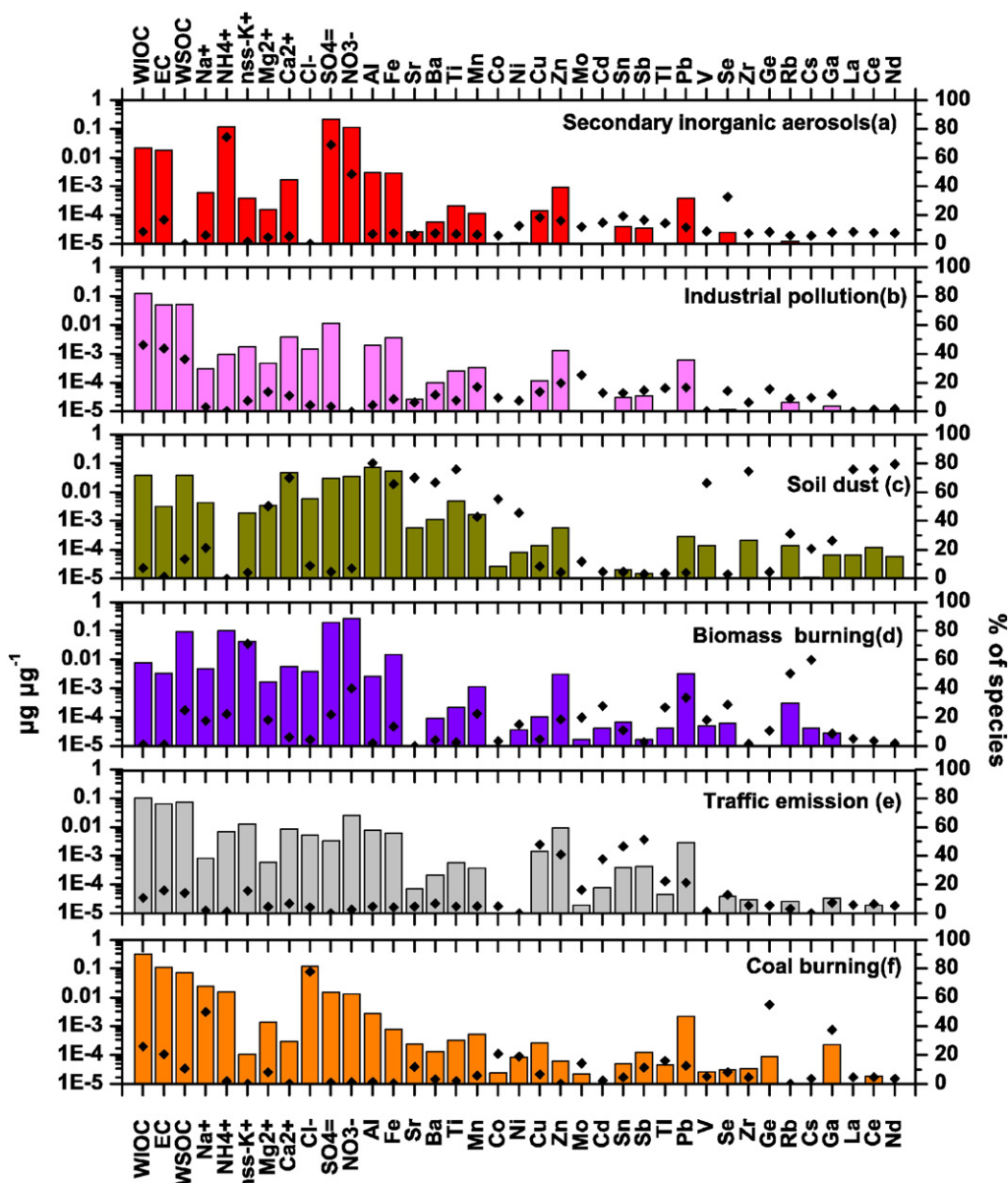


Fig. 3. Source profiles of  $PM_{2.5}$  with  $nss\text{-K}^+$  as a biomass burning tracer.

this season. Photochemistry could be very active in spring as suggested in other places (Zhang et al., 2008). Seasonal O<sub>3</sub> and NO<sub>2</sub> data also supported this possibility (Table 1). O<sub>3</sub> in summer (75 ± 27 μg m<sup>-3</sup>) and spring (65 ± 16 μg m<sup>-3</sup>) did not differ much, but was much higher than that in autumn (18 ± 9 μg m<sup>-3</sup>) and winter (17 ± 14 μg m<sup>-3</sup>). Although NO<sub>2</sub> was higher in autumn (67 ± 26 μg m<sup>-3</sup>) and winter (64 ± 45 μg m<sup>-3</sup>) than that in spring (49 ± 18 μg m<sup>-3</sup>) and summer (40 ± 10 μg m<sup>-3</sup>), the magnitude of the seasonal difference was small. Furthermore, O<sub>x</sub> (= O<sub>3</sub> + NO<sub>2</sub>) was the same in spring (114 μg m<sup>-3</sup>) and summer (115 μg m<sup>-3</sup>). Thus, LG degradation was likely the major cause of the differences in the analysis results between using LG and nss-K<sup>+</sup>. In general, biomass burning was likely important sources of carbonaceous aerosols in all of the seasons except in summer.

3.3. Comparison of source profiles of PM<sub>2.5</sub> based on two single and one combined tracers

Discussions in Section 3.2 suggest that using different tracers in PMF analysis might provide different source attributions to PM<sub>2.5</sub>. To confirm this assumption, three biomass burning tracers, nss-K<sup>+</sup>, LG, and a

combination of nss-K<sup>+</sup> and LG, were applied to PMF analysis separately to generate three sets of source profiles (Fig. 3, Figs. 4 and 5). As expected, the identified source profiles of biomass burning differed significantly when using different biomass burning tracers. However, source profiles including biomass burning are similar using LG and combined LG and nss-K<sup>+</sup>. Those from using nss-K<sup>+</sup> were characterized by high WSOC, nss-K<sup>+</sup>, NO<sub>3</sub><sup>-</sup>, Rb and Cs concentrations (Fig. 3) while those from using LG or combined LG and nss-K<sup>+</sup> were characterized by high concentrations of WIOC, EC, WSOC and LG (Figs. 4 and 5). The major differences between the three sets of source profiles were reflected in the significantly different contents of NO<sub>3</sub><sup>-</sup>, WIOC and EC, which were the dominant chemical components of PM<sub>2.5</sub>. In all of the cases, WSOC was an important component of biomass burning source profiles and had similar concentration levels (0.16, 0.11 and 0.12 μg μg<sup>-1</sup>, respectively) when using tracer nss-K<sup>+</sup>, LG and a combination of nss-K<sup>+</sup> and LG. These estimated numbers in Beijing were close to those measured in Chengdu in field biomass burning smoke (rape and wheat straws) (0.10–0.13) (Tao et al., 2013).

In the three sets of source profiles, secondary inorganic aerosol was characterized by high NH<sub>4</sub><sup>+</sup>, SO<sub>4</sub><sup>2-</sup> and NO<sub>3</sub><sup>-</sup>; industrial pollution was

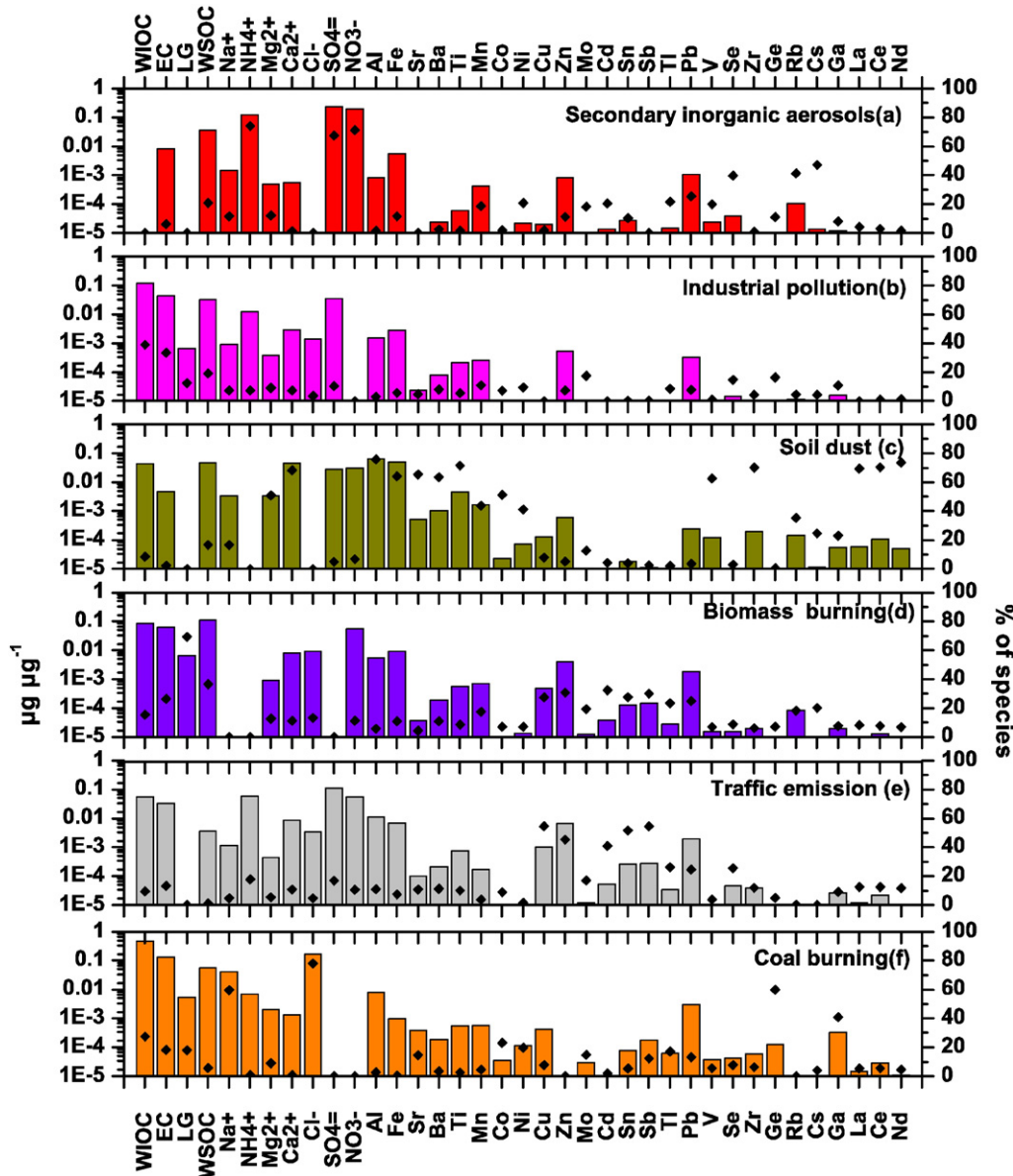


Fig. 4. Source profiles of PM<sub>2.5</sub> with LG as a biomass burning tracer.

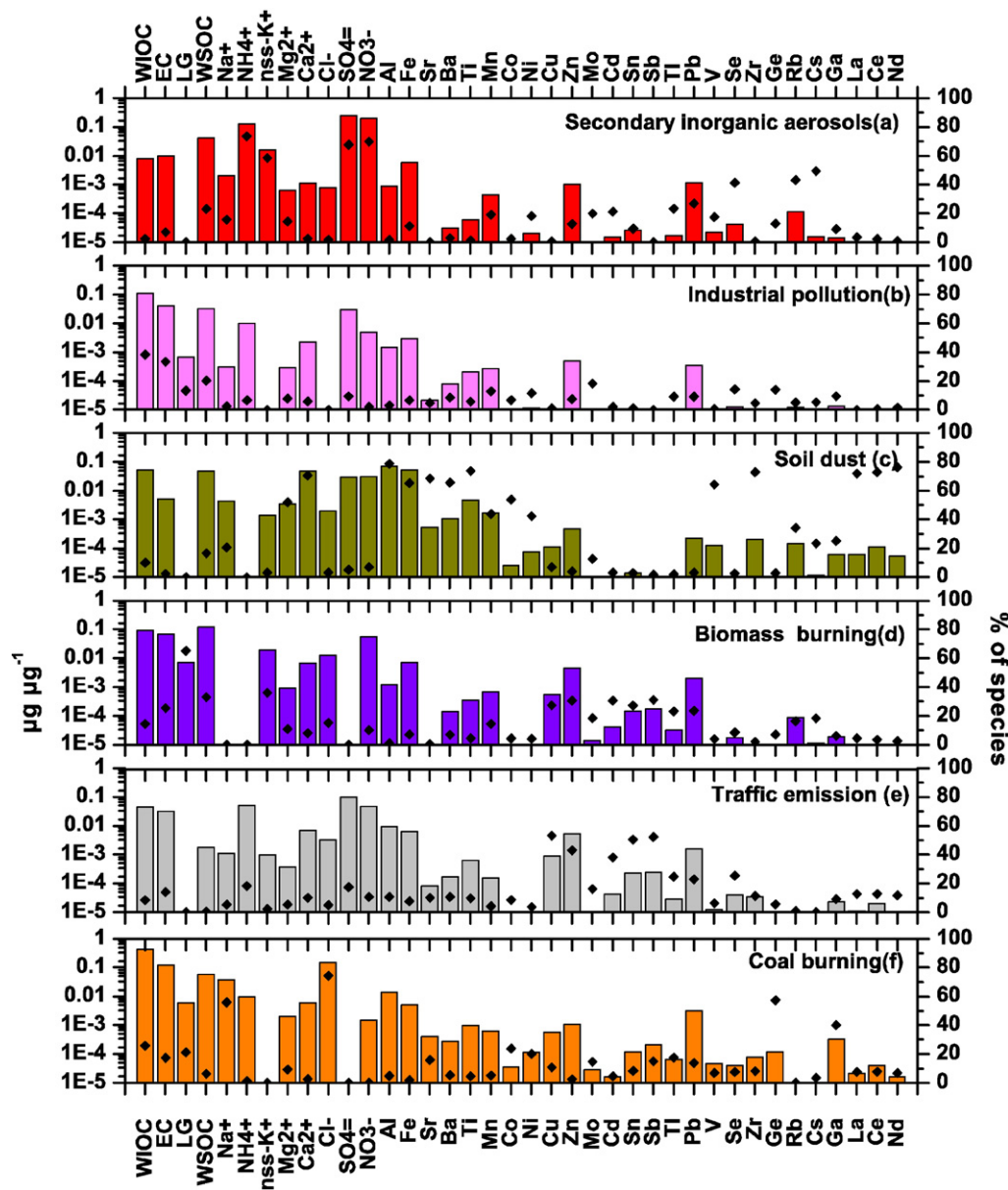


Fig. 5. Source profiles of  $PM_{2.5}$  with combined LG and  $nss-K^+$  as a biomass burning tracer.

characterized by high WIOC, WSOC and EC; soil dust was characterized by high  $Mg^{2+}$ ,  $Ca^{2+}$ , Al, Fe and other crustal elements; traffic emission was characterized by high Cu, Zn, Sn and Sb; and coal burning was characterized by high  $Na^+$ ,  $Cl^-$ , Ge and Ga (Zhang et al., 2013).

Coal burning is still one of the major energy sources in northern China, both in industry and in winter heating. Thus, industrial pollution should be one important source of carbonaceous aerosols, as shown in the high contents of WIOC, WSOC and EC in the source profiles. Although the coal burning source was also characterized by high WIOC, WSOC and EC, their contents were lower than those in industrial pollution. The contribution of coal burning to  $PM_{2.5}$  was evidently higher in winter than in other seasons, consistent with much higher  $SO_2$  concentrations in winter. The long lifetime of  $SO_2$  in winter due to low  $O_x$  concentration can only partially explain such high  $SO_2$  concentration, suggesting the existence of additional  $SO_2$  sources (Lee et al., 2011). Besides, a good relationship between  $SO_2$  and  $Cl^-$  was also found in winter (Zhang et al., 2013). Thus, coal burning defined in this study should be mainly related to heating activities instead of industrial combustion.

It is noted that source profile of biomass burning identified by using  $nss-K^+$  included abundant  $NO_3^-$ , which also existed in secondary

inorganic aerosol. The typical chemical components (e.g. WIOC, WSOC and EC) in source profiles of biomass burning identified by using LG and combined LG and  $nss-K^+$  were similar to those in industrial pollution. Thus, despite similar source profiles for the majority of sources generated from using  $nss-K^+$  or LG or combined LG and  $nss-K^+$  as a biomass burning tracer, quantification of source contributions could differ significantly, especially for secondary inorganic aerosol, industrial pollution, and biomass burning. As expected, good correlations ( $R^2$  ranged from 0.94 to 0.99) were found between the simulated  $PM_{2.5}$  components from the six sources when using LG and combined LG and  $nss-K^+$  (Fig. 6). However, poor correlations ( $R^2$  ranged from 0.02 to 0.63) were found between the simulated  $PM_{2.5}$  components from secondary inorganic aerosol, industrial pollution, biomass burning and traffic emission contributions when using LG and  $nss-K^+$  (Fig. 7). In contrast, good correlations ( $R^2 > 0.99$ ) were found for soil dust and coal burning.

The simulated industrial pollution, soil dust, and coal burning concentrations were similar when using LG and combined LG and  $nss-K^+$  as a tracer with the regression slopes close to 1.0. The regression slopes from the simulated secondary inorganic aerosol and biomass burning was 0.92 and 0.86, respectively, suggesting slightly higher contributions

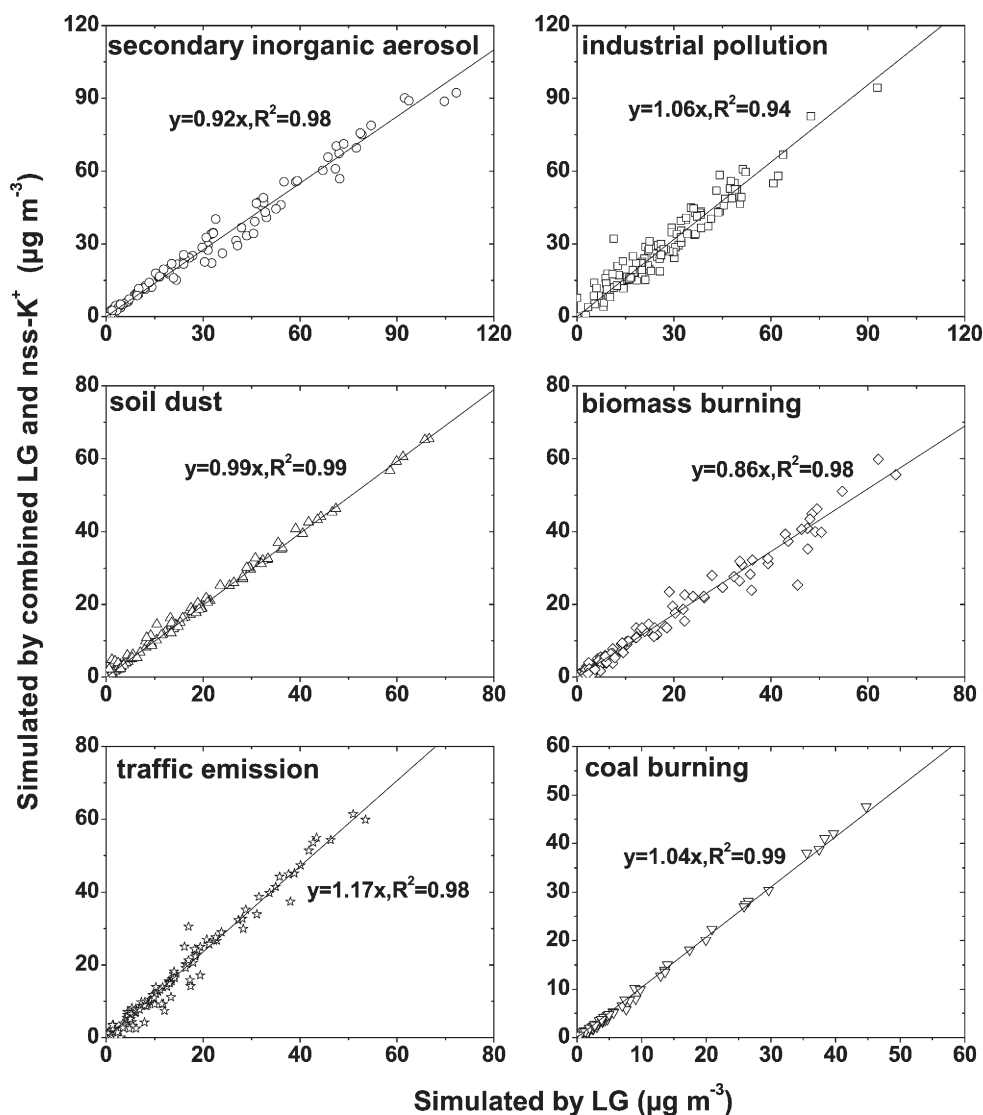


**Fig. 6.** Correlations of simulated source contributions (PM<sub>2.5</sub> mass concentration fractions from different sources) between those using combined LG and nss-K<sup>+</sup> and those using LG as a biomass burning tracer.

from these sources using LG as the tracer compared to using combined LG and nss-K<sup>+</sup>. The opposite trend was found from the simulated traffic emission with a slope of 1.17. Source attribution results from using nss-K<sup>+</sup> as a tracer differed significantly from those using LG or combined LG and nss-K<sup>+</sup>. For example, the regression slopes for the simulated sources between using nss-K<sup>+</sup> and LG varied greatly from 0.33 to 1.37. The largest uncertainties were for industrial pollution (a slope of 1.37), biomass burning (0.33) and traffic emission (0.36).

On an annual basis, the contributions to PM<sub>2.5</sub> from secondary inorganic aerosol, industrial pollution, soil dust, biomass burning, traffic emission and coal burning were estimated to be  $31 \pm 37\%$ ,  $39 \pm 28\%$ ,  $14 \pm 14\%$ ,  $7 \pm 7\%$ ,  $5 \pm 6\%$ , and  $4 \pm 8\%$ , respectively, using the nss-K<sup>+</sup> source profiles. If instead using LG or combined LG and nss-K<sup>+</sup> source profiles, up to 3% absolute percentage differences were found for all the sources. The differences can be much larger on seasonal basis, e.g., larger than 24% in at least one season for secondary inorganic aerosol, industrial pollution, biomass burning and traffic emission sources. Among all the sources, the largest uncertainties were for the estimation of secondary inorganic aerosol (10%) and industrial pollution (10%) on annual basis and of industrial pollution (28%) on seasonal basis.

### 3.4. Contributions of biomass burning and other sources to WSOC

To investigate the uncertainties in the estimation of biomass burning contributions to WSOC, three sets of source profiles separately generated from using three different tracers were applied to apportion sources of WSOC. On an annual basis, the contributions of biomass burning sources to WSOC were estimated to be  $25 \pm 19\%$ ,  $28 \pm 23\%$ , and  $25 \pm 21\%$  using nss-K<sup>+</sup>, LG and combined LG and nss-K<sup>+</sup> source profiles, respectively. Seasonal contributions were slightly higher using nss-K<sup>+</sup> than using LG and combined LG and nss-K<sup>+</sup> in spring (38% versus 18% and 19%) and summer (24% versus 3% and 2%), and much lower in autumn (30% versus 54% and 49%) and winter (10% versus 34% and 27%). Thus, the uncertainties in the estimation of biomass burning contributions to WSOC were around 3% annually and up to 24% seasonally in terms of the absolute percentage contributions. These correspond to uncertainties of a factor of 1.7 annually and up to a factor of 3.3 seasonally in the estimated WSOC concentrations.

The uncertainties in the estimated contributions from the other five sources to WSOC were also investigated. On an annual basis, the contributions to WSOC from secondary inorganic aerosol, industrial pollution, soil dust, traffic emission, and coal burning were estimated to be  $0 \pm 0\%$ ,

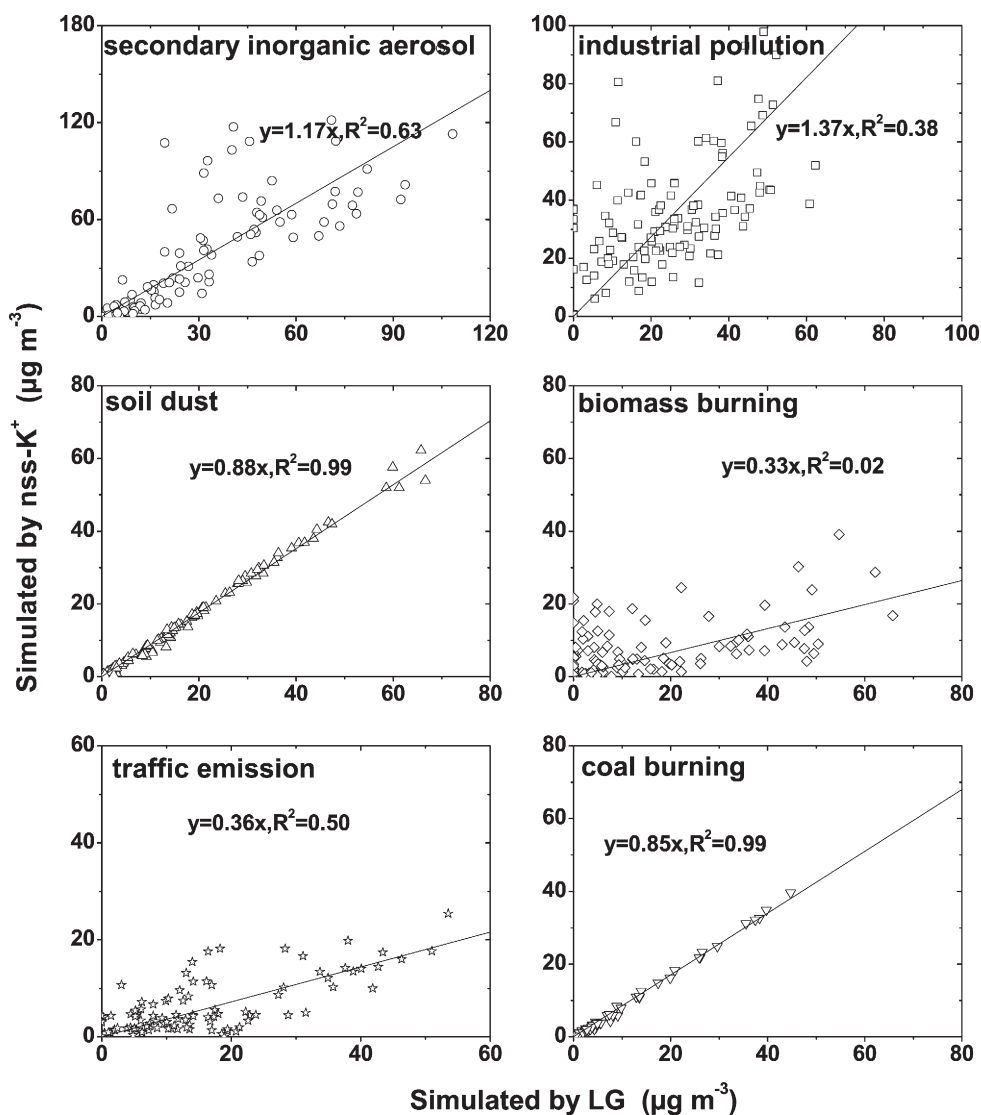


Fig. 7. Correlations of simulated source contributions (PM<sub>2.5</sub> mass concentration fractions from different sources) between those using nss-K<sup>+</sup> and those using LG as a biomass burning tracer.

41 ± 20%, 12 ± 13%, 9 ± 9% and 13 ± 17%, respectively, using the nss-K<sup>+</sup> source profiles, and the corresponding numbers are 22 ± 21%, 24 ± 18%, 20 ± 19%, 1 ± 1% and 5 ± 6% using the LG source profile, and are 23 ± 22%, 26 ± 19%, 20 ± 19%, 1 ± 1% and 5 ± 7% using the combined LG and nss-K<sup>+</sup> source profile. Up to 23% differences annually and 39% seasonally were found in terms of the absolute percentage contributions. For the major source - industrial pollution, the uncertainty represented a factor of 1.9 annually and up to a factor of 2.5 seasonally in the estimated WSOC concentrations.

#### 4. Conclusions

To investigate the sources of WSOC in PM<sub>2.5</sub>, WSOC and other major chemical components were measured in 2009–2010 at an urban site in Beijing. Annual mean concentration of WSOC was 6.4 ± 3.6 μgC m<sup>-3</sup> with a summer average (3.2 ± 1.1 μgC m<sup>-3</sup>) less than half of those in other seasons (6.7 ± 1.8 μgC m<sup>-3</sup> to 7.7 ± 5.0 μgC m<sup>-3</sup>). Source profiles generated from using LG as a biomass burning tracer differed slightly from those using combined tracers of LG and nss-K<sup>+</sup>; however, they both differed significantly from those using nss-K<sup>+</sup>. The differences in the absolute percentage

contributions to PM<sub>2.5</sub> estimated from using different tracers were smaller than 5% for all the sources. On an annual basis, the contributions of biomass burning sources to WSOC were estimated to be 25 ± 18%, 28 ± 23%, and 25 ± 21% using nss-K<sup>+</sup>, LG and combined LG and nss-K<sup>+</sup> source profiles, respectively, or around 3% differences. Seasonal differences were up to 24%. The large percentage difference in turn caused similar order of magnitude difference in the estimation of contribution from the industrial pollution to WSOC. The results presented in this study suggest that caution should be taken when selecting biomass burning tracers in source apportionment analysis using PMF. Improvements in PMF analysis technique are needed to reduce such large uncertainties in future studies.

#### Acknowledgments

This study was financially supported by the Special Scientific Research Funds for Environment Protection Commonwealth Section (No. 200809143), the National Natural Science Foundation of China (No. 41175131), and the Special Scientific Research Funds for National Basic Research Program of China (2013FY112700).

## References

- Ali-Mohamed, A.Y., 1991. Estimation of inorganic particulate matter in the atmosphere of Isa Town, Bahrain, by dry deposition. *Atmos. Environ.* 25, 397–405.
- Ali-Mohamed, A.Y., Ali, H.A., 2001. Estimation of atmospheric inorganic water-soluble particulate matter in Muharrag Island, Bahrain, (Arabian Gulf), by ion chromatography. *Atmos. Environ.* 35, 761–768.
- Andreae, M.O., 1983. Soot carbon and excess fine potassium: long-range transport of combustion-derived aerosols. *Science* 220, 1148–1151.
- Bell, M.L., Dominici, F., Ebisu, K., Zeger, S.L., Samet, J.M., 2007. Spatial and temporal variation in PM<sub>2.5</sub> chemical composition in the United States for health effects studies. *Environ. Health Perspect.* 989–995.
- Chan, C.K., Yao, X., 2008. Air pollution in mega cities in China. *Atmos. Environ.* 42, 1–42.
- Cheng, Y., Engling, G., He, K.B., Duan, F.K., Ma, Y.L., Du, Z.Y., Liu, J.M., Zheng, M., Weber, R.J., 2013. Biomass burning contribution to Beijing aerosol. *Atmos. Chem. Phys.* 13, 7765–7781.
- Cheng, Z., Lam, K., Chan, L., Wang, T., Cheng, K., 2000. Chemical characteristics of aerosols at coastal station in Hong Kong. I. Seasonal variation of major ions, halogens and mineral dusts between 1995 and 1996. *Atmos. Environ.* 34, 2771–2783.
- Decesari, S., Facchini, M., Mircea, M., Cavalli, F., Fuzzi, S., 2003. Solubility properties of surfactants in atmospheric aerosol and cloud/fog water samples. *J. Geophys. Res.* 108 (D21), 4685.
- Ding, X., Zheng, M., Yu, L., Zhang, X., Weber, R.J., Yan, B., Russell, A.G., Edgerton, E.S., Wang, X., 2008. Spatial and seasonal trends in biogenic secondary organic aerosol tracers and water-soluble organic carbon in the southeastern United States. *Environ. Sci. Technol.* 42, 5171–5176.
- Docherty, K.S., Stone, E.A., Ulbrich, I.M., DeCarlo, P.F., Snyder, D.C., Schauer, J.J., Peltier, R.E., Weber, R.J., Murphy, S.M., Seinfeld, J.H., 2008. Apportionment of primary and secondary organic aerosols in southern California during the 2005 study of organic aerosols in Riverside (SOAR-1). *Environ. Sci. Technol.* 42, 7655–7662.
- Du, Z., He, K., Cheng, Y., Duan, F., Ma, Y., Liu, J., Zhang, X., Zheng, M., Weber, R., 2014a. A yearlong study of water-soluble organic carbon in Beijing I: sources and its primary vs. secondary nature. *Atmos. Environ.* 92, 514–521.
- Du, Z., He, K., Cheng, Y., Duan, F., Ma, Y., Liu, J., Zhang, X., Zheng, M., Weber, R., 2014b. A yearlong study of water-soluble organic carbon in Beijing II: light absorption properties. *Atmos. Environ.* 89, 235–241.
- Duvall, R., Majestic, B., Shafer, M., Chuang, P., Simoneit, B., Schauer, J., 2008. The water-soluble fraction of carbon, sulfur, and crustal elements in Asian aerosols and Asian soils. *Atmos. Environ.* 42, 5872–5884.
- Fang, G.C., Liu, C.K., 2010. Ambient suspended particulate matter and ionic speciation in Asian countries during 1998–2007. *Toxicol. Ind. Health* 26, 589–600.
- Fraser, M.P., Lakshmanan, K., 2000. Using levoglucosan as a molecular marker for the long-range transport of biomass combustion aerosols. *Environ. Sci. Technol.* 34, 4560–4564.
- Gieré, R., Blackford, M., Smith, K., 2006. TEM study of PM<sub>2.5</sub> emitted from coal and tire combustion in a thermal power station. *Environ. Sci. Technol.* 40, 6235–6240.
- Gordon, T., Presto, A., May, A., Nguyen, N., Lipsky, E., Donahue, N., Gutierrez, A., Zhang, M., Maddox, C., Rieger, P., 2014. Secondary organic aerosol formation exceeds primary particulate matter emissions for light-duty gasoline vehicles. *Atmos. Chem. Phys.* 14, 4661–4678.
- Hecobian, A., Zhang, X., Zheng, M., Frank, N., Edgerton, E.S., Weber, R.J., 2010. Water-soluble organic aerosol material and the light-absorption characteristics of aqueous extracts measured over the southeastern United States. *Atmos. Chem. Phys.* 10, 5965–5977.
- Huang, H., Ho, K., Lee, S., Tsang, P., Ho, S.S.H., Zou, C., Zou, S., Cao, J., Xu, H., 2012. Characteristics of carbonaceous aerosol in PM<sub>2.5</sub>: Pearl Delta River region, China. *Atmos. Res.* 104, 227–236.
- Johansen, A.M., Hoffmann, M.R., 2004. Chemical characterization of ambient aerosol collected during the northeast monsoon season over the Arabian Sea: anions and cations. *J. Geophys. Res.* 109, D05305.
- Jung, J., Kim, Y.J., Aggarwal, S.G., Kawamura, K., 2011. Hygroscopic property of water-soluble organic-enriched aerosols in Ulaanbaatar, Mongolia during the cold winter of 2007. *Atmos. Environ.* 45, 2722–2729.
- Kalberer, M., Yu, J., Cocker, D., Flagan, R., Seinfeld, J.H., 2000. Aerosol formation in the cyclohexene-ozone system. *Environ. Sci. Technol.* 34, 4894–4901.
- Kumar, A., Mishra, M.K., Divkar, J., Rout, S., Narayanan, U., Hegde, A., 2010. Impact of particle size on distribution of major ions in acid- and water-soluble components of PM<sub>10</sub> atmospheric aerosols in the coastal region of Mumbai. *Atmos. Res.* 98, 406–415.
- Lee, C., Martin, R.V., van Donkelaar, A., Lee, H., Dickerson, R.R., Hains, J.C., Krotkov, N., Richter, A., Vinnikov, K., Schwab, J.J., 2011. SO<sub>2</sub> emissions and lifetimes: estimates from inverse modeling using in situ and global, space-based (SCIAMACHY and OMI) observations. *J. Geophys. Res.* 116, D06304.
- Ninomiya, Y., Zhang, L., Sato, A., Dong, Z., 2004. Influence of coal particle size on particulate matter emission and its chemical species produced during coal combustion. *Fuel Process. Technol.* 85, 1065–1088.
- Norris, G., Duvall, R., Brown, S., Bai, S., 2014. EPA positive matrix factorization (PMF) 5.0 fundamentals and user guide. US Environmental Protection Agency, Office of Research and Development, Washington, DC.
- Park, S.S., Cho, S.Y., Kim, K.W., Lee, K.H., Jung, K., 2012. Investigation of organic aerosol sources using fractionated water-soluble organic carbon measured at an urban site. *Atmos. Environ.* 55, 64–72.
- Pathak, R.K., Wang, T., Ho, K., Lee, S., 2011. Characteristics of summertime PM<sub>2.5</sub> organic and elemental carbon in four major Chinese cities: implications of high acidity for water-soluble organic carbon (WSOC). *Atmos. Environ.* 45, 318–325.
- Peltier, R.E., Sullivan, A., Weber, R., Wollny, A., Holloway, J., Brock, C., De Gouw, J., Atlas, E., 2007. No evidence for acid-catalyzed secondary organic aerosol formation in power plant plumes over metropolitan Atlanta, Georgia. *Geophys. Res. Lett.* 34, L06801.
- Popovicheva, O., Kistler, M., Kireeva, E., Persiantseva, N., Timofeev, M., Kopeikin, V., Kasper-Giebl, A., 2014. Physicochemical characterization of smoke aerosol during large-scale wildfires: extreme event of August 2010 in Moscow. *Atmos. Environ.* 96, 405–414.
- Ram, K., Sarin, M., 2011. Day-night variability of EC, OC, WSOC and inorganic ions in urban environment of indo-gangetic plain: implications to secondary aerosol formation. *Atmos. Environ.* 45, 460–468.
- Seinfeld, J.H., Carmichael, G.R., Arimoto, R., Conant, W.C., Brechtel, F.J., Bates, T.S., Cahill, T.A., Clarke, A.D., Doherty, S.J., Flatau, P.J., 2004. ACE-ASIA-regional climatic and atmospheric chemical effects of Asian dust and pollution. *Bull. Am. Meteorol. Soc.* 85, 367–380.
- Sullivan, A., Peltier, R.E., Brock, C., De Gouw, J., Holloway, J., Warneke, C., Wollny, A., Weber, R., 2006. Airborne measurements of carbonaceous aerosol soluble in water over northeastern United States: method development and an investigation into water-soluble organic carbon sources. *J. Geophys. Res.* 111, D23546.
- Tao, J., Gao, J., Zhang, L., Zhang, R., Che, H., Zhang, Z., Lin, Z., Jing, J., Cao, J., Hsu, S.C., 2014. PM<sub>2.5</sub> pollution in a megacity of southwest China: source apportionment and implication. *Atmos. Chem. Phys.* 14, 8679–8699.
- Tao, J., Zhang, L., Engling, G., Zhang, R., Yang, Y., Cao, J., Zhu, C., Wang, Q., Luo, L., 2013. Chemical composition of PM<sub>2.5</sub> in an urban environment in Chengdu, China: importance of springtime dust storms and biomass burning. *Atmos. Res.* 122, 270–283.
- Timonen, H., Aurela, M., Carbone, S., Saarnio, K., Saarikoski, S., Mäkelä, T., Kulmala, M., Kerminen, V.-M., Worsnop, D., Hillamo, R., 2010. High time-resolution chemical characterization of the water-soluble fraction of ambient aerosols with PILS-TOC-IC and AMS. *Atmos. Meas. Tech.* 3, 1063–1074.
- Viana, M., Maenhaut, W., Ten Brink, H., Chi, X., Weijers, E., Querol, X., Alastuey, A., Mikuška, P., Večeřa, Z., 2007. Comparative analysis of organic and elemental carbon concentrations in carbonaceous aerosols in three European cities. *Atmos. Environ.* 41, 5972–5983.
- Wang, G., Huang, L., Gao, S., Gao, S., Wang, L., 2002. Characterization of water-soluble species of PM<sub>10</sub> and PM<sub>2.5</sub> aerosols in urban area in Nanjing, China. *Atmos. Environ.* 36, 1299–1307.
- Wang, Q., Shao, M., Liu, Y., William, K., Paul, G., Li, X., Liu, Y., Lu, S., 2007. Impact of biomass burning on urban air quality estimated by organic tracers: Guangzhou and Beijing as cases. *Atmos. Environ.* 41, 8380–8390.
- Watson, J.G., Chow, J.C., Houck, J.E., 2001. PM<sub>2.5</sub> chemical source profiles for vehicle exhaust, vegetative burning, geological material, and coal burning in Northwestern Colorado during 1995. *Chemosphere* 43, 1141–1151.
- Wonaschütz, A., Hersey, S., Sorooshian, A., Craven, J., Metcalf, A., Flagan, R., Seinfeld, J., 2011. Impact of a large wildfire on water-soluble organic aerosol in a major urban area: the 2009 station fire in Los Angeles county. *Atmos. Chem. Phys.* 11, 8257–8270.
- Zhang, T., Cao, J., Tie, X., Shen, Z., Liu, S., Ding, H., Han, Y., Wang, G., Ho, K., Qiang, J., 2011a. Water-soluble ions in atmospheric aerosols measured in Xi'an, China: seasonal variations and sources. *Atmos. Res.* 102, 110–119.
- Zhang, Z., Gao, J., Engling, G., Tao, J., Chai, F., Zhang, L., Zhang, R., Sang, X., Chan, C., Lin, Z., 2015. Characteristics and applications of size-segregated biomass burning tracers in China's Pearl River Delta region. *Atmos. Environ.* 102, 290–301.
- Zhang, R., Jing, J., Tao, J., Hsu, S.C., Wang, G., Cao, J., Lee, C.S.L., Zhu, L., Chen, Z., Zhao, Y., Shen, Z., 2013. Chemical characterization and source apportionment of PM<sub>2.5</sub> in Beijing: seasonal perspective. *Atmos. Chem. Phys.* 13, 7053–7074.
- Zhang, X., Lin, Y.H., Surratt, J.D., Zotter, P., Prévôt, A.S., Weber, R.J., 2011b. Light-absorbing soluble organic aerosol in Los Angeles and Atlanta: a contrast in secondary organic aerosol. *Geophys. Res. Lett.* 38, L21810.
- Zhang, L., Wiebe, A., Vet, R., Mihele, C., O'Brien, J.M., Iqbal, S., Liang, Z., 2008. Measurements of reactive oxidized nitrogen at eight Canadian rural sites. *Atmos. Environ.* 42, 8065–8078.
- Zhao, X., Zhang, X., Xu, X., Xu, J., Meng, W., Pu, W., 2009. Seasonal and diurnal variations of ambient PM<sub>2.5</sub> concentration in urban and rural environments in Beijing. *Atmos. Environ.* 43, 2893–2900.